

UniSTD: Towards Unified Spatio-Temporal Learning across Diverse Disciplines

Chen Tang¹ Xinzhu Ma^{1,2,*} Encheng Su² Xiufeng Song^{2,3} Xiaohong Liu³
 Wei-Hong Li^{1,4} Lei Bai² Wanli Ouyang^{1,2} Xiangyu Yue^{1,4,*}

¹MMLab, The Chinese University of Hong Kong

²Shanghai AI Lab

³Shanghai Jiaotong University

⁴Shun Hing Institute of Advanced Engineering, The Chinese University of Hong Kong

Abstract

Traditional spatiotemporal models generally rely on task-specific architectures, which limit their generalizability and scalability across diverse tasks due to domain-specific design requirements. In this paper, we introduce **UniSTD**, a unified Transformer-based framework for spatiotemporal modeling, which is inspired by advances in recent foundation models with the two-stage pretraining-then-adaption paradigm. Specifically, our work demonstrates that task-agnostic pretraining on 2D vision and vision-text datasets can build a generalizable model foundation for spatiotemporal learning, followed by specialized joint training on spatiotemporal datasets to enhance task-specific adaptability. To improve the learning capabilities across domains, our framework employs a rank-adaptive mixture-of-expert adaptation by using fractional interpolation to relax the discrete variables so that can be optimized in the continuous space. Additionally, we introduce a temporal module to incorporate temporal dynamics explicitly. We evaluate our approach on a large-scale dataset covering 10 tasks across 4 disciplines, demonstrating that a unified spatiotemporal model can achieve scalable, cross-task learning and support up to 10 tasks simultaneously within one model while reducing training costs in multi-domain applications. Code will be available at <https://github.com/1hunters/UniSTD>.

1. Introduction

In recent years, substantial progress has been made across a wide array of computer vision tasks, including image classification [7, 17, 59], object detection [18, 47, 81], and more [19, 30, 34, 52]. Among these, spatiotemporal learning—which focuses on predicting future events based on historical data—has emerged as crucial for numerous fields and practical applications, such as human motion prediction, traffic management, robotic planning,

*Corresponding Author

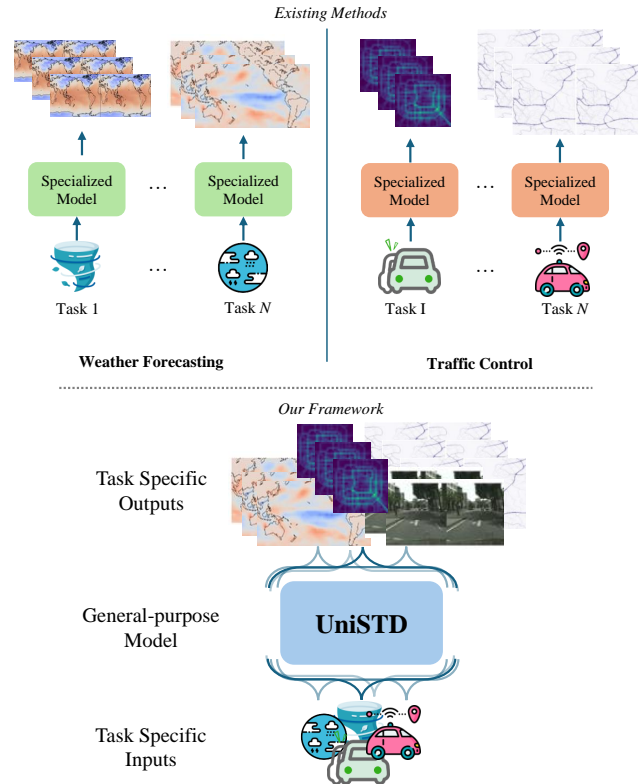


Figure 1. **Top:** Existing works need specialized models for both tasks within the same disciplines (e.g., weather forecasting, traffic control). **Bottom:** Unified Spatio-Temporal Learning. UniSTD unifies 4 disciplines with 10 tasks under one model and is trained on a massive collection of datasets.

weather forecasting, *etc.* By capturing both spatial correlations and temporal dynamics, spatiotemporal learning offers a robust framework for modeling the complexities of the physical world, enabling more accurate and responsive predictions in diverse, real-world contexts. While achieving meaningful progress, most of the existing methods [2, 10, 15, 28, 51, 57, 64, 65, 68–72, 75] still resort to designing specialized architectures to learn the spatiotemporal representations for each task.

Recurrent-based approaches have traditionally relied on Long Short-Term Memory (LSTM) networks [20] for se-

quential modeling. ConvLSTM [51] pioneered the application of convolutional LSTM networks for spatiotemporal predictive learning, it extends fully connected LSTM to incorporate convolutional layers. PredRNN [68] introduced Spatiotemporal LSTM (ST-LSTM) units, enabling a unified memory pool to capture both spatial appearances and temporal dynamics. Furthermore, E3D-LSTM [70] integrated 3D convolutional networks within LSTM units, facilitating robust representations that capture both short-term frame dependencies and long-term structural relationships. In contrast, *recurrent-free approaches* have emerged to circumvent iterative temporal predictions. Instead of generating temporal sequences incrementally, these methods simultaneously produce spatial and temporal predictions. SimVP [11] and SimVPv2 [56] employed a CNN backbone as a feature translator within an Encoder-Decoder framework. Earthformer [10] decomposes data into cuboidal regions to parallelize spatiotemporal forecasting for earth system applications. TAU [57] further explores generalized architectures by introducing the Temporal Attention Unit.

While effective in eliminating recursion, existing methods primarily focus on re-engineering architectures to tackle specific tasks. In other words, these models are each designed for a *single* task, heavily relying on task-specific domain knowledge [10]. Consequently, they suffer from unstable performance when they are directly applied to other tasks [58, 73], limiting their generality and inevitably leading to expensive computational and memory cost. This leads us to pose a critical, yet challenging question:

Can we comprehensively address diverse spatiotemporal domains with a single, universal framework?

A model with such generality would offer several distinct advantages: (i) it allows the usage of standard network architecture (e.g., Transformer) and hence enables the integration of extensive pretrained knowledge from widely available open-source weights within the research community, (ii) joint training across multiple spatiotemporal tasks could promote cross-task learning benefits, and (iii) It enhances scalability and operational efficiency for large-scale deployments, where simultaneous processing of tasks across various domains is required. The comparison between existing works and the proposed method is shown in Fig. 1.

To unify the diverse data patterns of spatiotemporal tasks within a single model, inspired by recent advances in large language models (LLMs) [3, 44, 45] and vision-language models (VLMs) [16, 35, 40]—where a well-pretrained Transformer can serve as a universal encoder for further multi-modal multi-task fine-tuning—we frame spatiotemporal learning as a two-stage optimization problem. Since transformers has been standard blocks for various modalities, e.g., vision and text, we employ a standard transformer model to build a generalizable architecture, and

further demonstrate that this choice allows us to leverage the extensive knowledge embedded in large-scale, task-agnostic pretraining on datasets such as 2D vision data and image-text pairs (e.g., OpenCLIP-ViT [24] and ImageNet-ViT [7]). In the second stage, which is the main focus of this paper, we perform joint training on the single model using task-specific spatiotemporal datasets for embedding domain-specific knowledge into the model, to fit the spatiotemporal tasks and improve the adaptability of the model.

Despite the promising prospect, performing joint training on a single model is extremely challenging due to the intricate properties of diverse disciplines (e.g., weather forecasting vs. traffic control), easily triggering conflicts between disciplines and resulting in sub-optimal convergence. To address this with minimal training cost, we propose a rank-adaptive Mixture-of-Experts (MoE) mechanism that dynamically optimizes low-rank adapter ranks based on task properties and interdependencies while selectively activating adapters according to input characteristics. To mitigate the complexity of rank optimization, we reformulate the problem using an auxiliary matrix-based approach, which reduces complexity and enables fine-grained rank adjustments. Our method achieves full differentiability by incorporating a continuous relaxation of discrete rank values, facilitating efficient optimization with minimal computational overhead. Additionally, to imbue models originally trained on 2D data with temporal awareness without introducing substantial computational overhead, we design a lightweight temporal module that incorporates zero-initialized projection MLP layers. This design eliminates the need to fine-tune the transformer’s computationally intensive FFN layers, thereby enhancing temporal modeling capabilities while maintaining efficiency.

Based on OpenSTL [58] and PredBench [73], we create a large-scale dataset encompassing 4 representative disciplines with a total of 10 tasks to support the joint training. Extensive experiments demonstrate the effectiveness of the proposed method, UniSTD achieves lossless performance when scaling up the number of tasks. Specifically, the existing methods have encountered significant performance drops at only 3 tasks jointly trained together, while at that time, UniSTD has up to 18.8 PSNR advanced compared to existing methods. The overall framework of UniSTD is shown in Fig. 2.

In summary, we make the following contributions:

- We introduce a unified framework for spatiotemporal modeling using a standard Transformer pretrained on task-agnostic datasets (e.g., OpenCLIP-ViT, ImageNet-ViT) and support specialized training on diverse spatiotemporal tasks, ensuring consistent performance, cross-task learning, and scalability with minimal reliance on domain-specific design.
- We decouple spatiotemporal modeling via rank-adaptive

MoEs and a lightweight temporal module, enabling efficient representation of spatial and temporal dependencies.

- Supported by a large-scale benchmark spanning four disciplines and ten tasks, UniSTD shows impressive performance in scaling the number of tasks without performance degradation, achieving up to 18.8 PSNR improvement compared to the current methods.

2. Related Work

2.1. Spatiotemporal Predictive Learning

Recurrent-based methods. Early works mainly focus on designing recurrent-based models for spatiotemporal predictive learning. ConvLSTM [51] integrates convolutional networks into LSTM architectures for better spatiotemporal modeling. PredNet [41] predicts future frames using deep recurrent convolutional networks with bidirectional connections. PredRNN [68] introduces a Spatiotemporal LSTM unit for joint spatial-temporal representation learning. E3D-LSTM [70] incorporates eidetic memory in recurrent units, and Conv-TT-LSTM [54] leverages higher-order ConvLSTMs to combine features across time. MotionRNN [74] highlights motion trends, while LMC-Memory [33] uses memory alignment for long-term motion context. PredRNN-v2 [72] further refines PredRNN with memory decoupling loss and curriculum learning.

Recurrent-free methods. Recurrent-free methods aim to address the inefficiency of recurrent models. SimVP [11] and SimVPv2 [56] adopt Inception-UNet blocks to down-sample the video sequences and learn spatiotemporal dynamics jointly, and then perform upsampling for prediction. While effective, convolutional methods struggle with long-term dependencies. MCVD [66] proposes a Masked Conditional Video Diffusion framework that uses the conditional video diffusion model based on the past-masking mechanism. TAU [57] replaces Inception-UNet with efficient attention modules, enabling parallelization and improved long-term temporal learning. Furthermore, WaST [43] adopts a 3D discrete wavelet transform module to extract low and high-frequency components jointly for better long-term dependency modeling. EarthFormer [10] leverages the space-time attention block for earth system forecasting, which decomposes the input into cuboids and then applies cuboid-level attention in parallel. Despite their promising performance, existing methods primarily focus on designing specialized architectures to tackle single spatiotemporal tasks. In this paper, we propose a general and scalable model based on a pure Transformer architecture to enable unified spatiotemporal learning.

2.2. General-purpose Model

Numerous efforts [4, 48, 61] have been made to develop a general-purpose model capable of handling diverse tasks

in a unified framework. Early works in the field of natural language processing (NLP) [3, 26, 29] and computer vision (CV) [31, 36, 37, 42, 79] demonstrated the feasibility of designing a unified framework to handle cross-task prediction or generation. ExT5 [1], UniT [23], and OFA [67] further demonstrate the large-scale multi-task joint training is of importance to the performance. UniHead [39], UniHCP [5], and UViM [32] leverage unified architectures (typically Transformer) to learn the shared representations for multiple perception vision tasks. Emu [55], SEED [13], and Mini-gemini [38] leverage both vision-language models and diffusion models to achieve text and visual generation. However, these methods do not focus on spatiotemporal learning, which has more diversity between tasks.

3. Method

3.1. Unified Modeling with Transformer

Preliminary. Spatiotemporal learning aims to infer the future frames using the previous ones. For a model that simultaneously supports M spatiotemporal tasks, each task i takes a sequence of historical information and predicts the future sequence. More formally, $\mathbf{X}_{T_i}^{(i)} = \{\mathbf{x}_j\}_{t-T_i+1}^t$ at time t with the past T frames, the output is $\mathbf{Y}_{T'_i}^{(i)} = \{\mathbf{y}_j\}_t^{t+T'_i}$ that contains the next T' frames, where $\mathbf{y}_j \in \mathbb{R}^{C_i \times H_i \times W_i}$ is an input with channels C_i , height H_i , and width W_i . Overall, the model is optimized by:

$$\Theta^* = \arg \min_{\Theta} \mathcal{L}_{\text{MSE}}(\mathcal{F}_{\Theta}(\mathbf{X}), \mathbf{Y}), \quad (1)$$

where Θ is the parameters of the model, $\mathbf{X} = \{\mathbf{X}_{T_i}^{(i)}\}_{i=1}^M$, \mathcal{L}_{MSE} denotes the mean squared error loss function. \mathcal{F}_{Θ} denotes the standard Transformer model [62] that alternates between Multi-Head Attention (MSA) and Feed-Forward Networks (FFN). The attention mechanism for each head is defined as:

$$\text{Attention}(\mathbf{Q}, \mathbf{K}, \mathbf{V}) = \text{Softmax}\left(\frac{\mathbf{Q}\mathbf{K}^{\top}}{\sqrt{L}}\right)\mathbf{V}, \quad (2)$$

where in self-attention, the queries \mathbf{Q} , keys \mathbf{K} , and values \mathbf{V} are linear projections of the input \mathbf{x} , represented as $\mathbf{Q} = \mathbf{x}\mathbf{W}^Q$, $\mathbf{K} = \mathbf{x}\mathbf{W}^K$, and $\mathbf{V} = \mathbf{x}\mathbf{W}^V$, with $\mathbf{x} \in \mathbb{R}^{N \times L}$; and $\mathbf{Q}, \mathbf{K}, \mathbf{V} \in \mathbb{R}^{L \times L}$, where N denotes the number of tokens, L is the hidden embedded dimension of Transformer. A linear layer then projects the output of self-attention. The FFN then processes each position in the sequence by applying two linear transformations:

$$\mathbf{Y} = \text{FFN}(\text{LN}(\mathbf{x})) + \mathbf{x}. \quad (3)$$

Encoder and Decoder architectures. In the encoder, we employ a canonical design in spatiotemporal representation learning [57], which incorporates a series

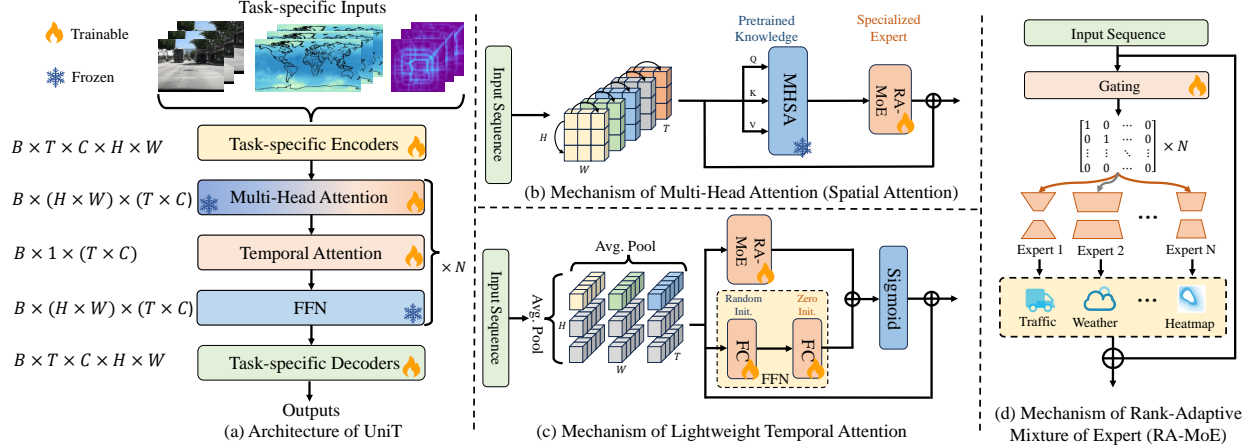


Figure 2. **Illustration of UniSTD.** Our method supports unified and scalable spatiotemporal learning across diverse disciplines. To achieve this, we use a standard Transformer to serve as the backbone, allowing us to take advantage of the pretrained weights from large-scale task-agnostic pertaining. Furthermore, to better embed the domain-specific knowledge into the model, we design a rank-adaptive MoE mechanism that dynamically adjusts the sub-architectures of model according to the joint training process, and a lightweight temporal attention module to explicitly capture the temporal dynamics.

of 2DConv-GroupNorm-SiLU layers to progressively downsample the spatial dimensions of the input. Given an input tensor with the shape $(B \times T_i) \times C_i \times H_i \times W_i$, where B denotes the batch size and T_i is folded into the batch dimension, the encoder produces an output with reduced spatial dimensions H'_i and W'_i , and an updated channel dimension C'_i , *i.e.*, the shape is $(B \times T_i) \times C'_i \times H'_i \times W'_i$. Then, it is reshaped into $B \times N \times L$ to serve as input to the Transformer, where $N = H'_i \times W'_i$ represents the spatial token count, and $L = T_i \times C'_i$ corresponds to the feature dimensionality of each token.

In the decoder, we apply an inverse process to that of the encoder. The output of the Transformer, initially in the shape $B \times N \times L$, is first reshaped to match the input format of the Transformer, specifically $(B \times T_i) \times C'_i \times H'_i \times W'_i$. It is then upsampled along the spatial dimension using transposed convolution.

Position Encoding. We adopt sinusoidal position encoding (SPE) generated with absolute coordinates for each patch, instead of learnable position embeddings used in existing Transformer models (*e.g.*, ViT, GPT).

Initialization. As discussed previously, pretrained Transformers provide strong modality adaption capability for various tasks (*e.g.*, 2D vision, vision-language understanding, *etc.*), we initialize the Transformer backbone (except for the task-specific encoder and decoder) with the pretrained weights.

3.2. Specialized Training

Although the standard Transformer allows us to use the weights on task-agnostic pertaining, we still need to perform specialized training for task-specific adaptability. However, with the remarkable scalability of modern Trans-

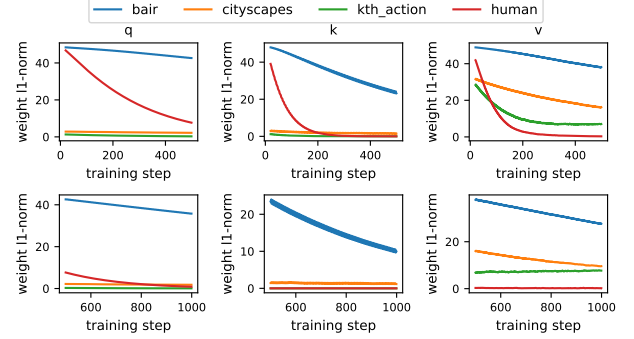


Figure 3. Weight updating patterns of task-specialized experts during optimization. We demonstrate the L1-norm of queries (Q), keys (K), and values (V) as a measurement for the optimal rank of each expert.

former models, the size of pre-trained models is increasing exponentially to achieve superior performance. As a result, the storage cost of the full training paradigm becomes prohibitive in multi-task scenarios [21, 27]. Therefore, we implement the specialized training with low-rank adaptation (LoRA) [21], which is a parameter-efficient finetuning technique that can reduce the number of fine-tuning parameters and memory usage. Specifically, given an input $\mathbf{x} \in \mathbb{R}^{N \times L}$, and original frozen weights $\mathbf{W}^{Q/K/V}$ in the multi-head self-attention layers, the low-rank adapter consist of two low-rank trainable matrices $\mathbf{A} \in \mathbb{R}^{L \times r'}$ and $\mathbf{B} \in \mathbb{R}^{r' \times L}$, where $r' \ll L$:

$$\mathbf{Y}_{r'}^{Q/K/V} = \mathbf{x} \underbrace{\mathbf{W}^{Q/K/V}}_{\text{frozen}} + \alpha \cdot \mathbf{x} \underbrace{\mathbf{A}_{r'} \mathbf{B}_{r'}}_{\text{trainable}} \quad (4)$$

Rank-adaptive MoE. As shown in Fig. 3, we have observed that tasks have quite discrepant update patterns of

the weight, this suggests making all tasks share a *single* low-rank adapter is easy to yield sub-optimal performance. Therefore, to effectively balance multi-spatiotemporal tasks spanning diverse disciplines with highly distinct characteristics (e.g., weather, traffic, etc.), we employ the mixture-of-experts paradigm. Specifically, a dynamic router $\mathcal{G}(\cdot)$ is utilized to adaptively assign weights w to low-rank adapters based on the requirements of the specific input task/discipline. For low-rank adapter in l -th layer, Eq. (4) becomes:

$$\mathbf{Y}_{r'}^{Q/K/V} = \mathbf{x} \underbrace{\mathbf{W}^{Q/K/V}}_{\text{frozen}} + \alpha \cdot \sum_{i=1}^N \mathbf{x} \underbrace{\mathcal{G}^{(i)}(\mathbf{x}) \mathbf{A}_{r'}^{(i)} \mathbf{B}_{r'}^{(i)}}_{\text{trainable}}, \quad (5)$$

where $\mathcal{G}^{(i)}(\cdot)$ denotes the i -th component.

Fig. 3 illustrates that \mathbf{Q} , \mathbf{K} , and \mathbf{V} exhibit task-specific weight update patterns, implying that *the rank r' of each expert should be dynamically adjusted based on task properties and interdependencies*, rather than being fixed or pre-defined. However, direct optimization of the discrete rank r' poses a combinatorial challenge. Considering a low-rank MoE model of 10 layers, with each layer containing 5 experts, and 4 potential rank configurations for each expert, the dimensionality of the search space dramatically explodes to $4^{5 \times 10}$. This exponential growth is computationally prohibitive, as each expert requires independent storage for its rank configurations. Additionally, an exhaustive brute-force search over this space is computationally infeasible.

In addressing this issue, we first convert the original form to an equivalent form from the perspective of the block matrix and use a new identity matrix $\mathbf{I}_{r-1,r}$, where r is an arbitrary rank of \mathbf{A} and \mathbf{B} to serve as the maximum of the rank:

$$\begin{aligned} (\mathbf{AB})_{r-1} &= \mathbf{A} \mathbf{I}_{r-1,r} \mathbf{B} = [\mathbf{a}_1 \quad \cdots \quad \mathbf{a}_r] \mathbf{I}_{r-1,r} \begin{bmatrix} \mathbf{b}_1 \\ \vdots \\ \mathbf{b}_r \end{bmatrix}, \\ \text{where } \mathbf{I}_{r-1,r} &= \begin{bmatrix} 1 & 0 & \cdots & 0 \\ 0 & 1 & \cdots & 0 \\ 0 & 0 & \cdots & 0 \\ \vdots & \vdots & \ddots & \vdots \\ 0 & 0 & \cdots & 0 \end{bmatrix}_{r \times r}. \end{aligned} \quad (6)$$

Here, we omit the index of expert and the rank r for simplicity. To be precise, $\mathbf{I}_{r-1,r}$ represents a modified $r \times r$ identity matrix, where the first $r - 1$ diagonal elements are 1, and the remaining $r - (r - 1)$ diagonal elements are 0. Utilizing block matrix multiplication, it can be demonstrated that the rank of $(\mathbf{BA})_{r-1}$ is reduced to $r - 1$. For any $1 \leq k < r$, it is trivial to build a rank $r - k$ solution according to Eq. (6). Unlike the original form that requires storing K copies for one expert, this new form allows for precise control of the

rank by constraining the number of nonzero elements on the main diagonal of the original identity matrix.

However, the new form still explicitly needs a discrete k to acquire the rank, which is non-differentiable for optimization. Then, we consider using relaxation to make it continuous by leveraging the fact that any continuous value is between its two adjacent discrete values. Specifically, we define the continuous rank from the integer domain as follows:

$$f_r(\mathbf{x}) \triangleq ([r] - r)g_{[r]}(\mathbf{x}) + (r - [r])g_{[r]}(\mathbf{x}),$$

$$\text{where } g_*(\mathbf{x}) = \begin{cases} \mathbf{x} \mathbf{A} \mathbf{I}_n [: [r]] \mathbf{B} & \text{if } * \text{ is } [r] \\ \mathbf{x} \mathbf{A} \mathbf{I}_n [: [r]] \mathbf{B} & \text{if } * \text{ is } [r] \end{cases} \quad (7)$$

It is clear that if the output of $f_r(\mathbf{x})$ is bounded by the two integer values of the rank r , i.e., $g_{[r]}(\mathbf{x}) \leq f_r(\mathbf{x}) \leq g_{[r]}(\mathbf{x})$. Substitute Eq. (7) into Eq. (5), we have:

$$\mathbf{Y}_r^{Q/K/V} = \mathbf{x} \mathbf{W}^{Q/K/V} + \alpha \cdot \sum_{i=1}^N \mathcal{G}^{(i)}(\mathbf{x}) f_r^{(i)}(\mathbf{x}). \quad (8)$$

Accordingly, the gradient of r is hereby defined by the difference of the upper bound and lower bound:

$$\frac{\partial f_r(\mathbf{x})}{\partial r} = \gamma \cdot (g_{[r]} - g_{[r]}), \quad (9)$$

where γ is a hyper-parameter to compensate the approximation error.

Once the rank r becomes continuous, another benefit is that we can directly restrict the additional trainable parameters for controlling the storage overhead, which is crucial otherwise the rank may become as large as possible. Specifically, we can control the expected size using the L1 distance to directly optimize the summed r of each expert. Therefore, the overall training objective is:

$$\mathcal{L} = \mathcal{L}_{\text{MSE}} + \beta \cdot \left| C - \sum_{i=1}^N r_i \right|, \quad (10)$$

where β is the hyper-parameter to weight the MSE loss and L1 loss, and C is the target size of summed LoRA modules. We use the first 10 epochs for optimizing the rank with rank-adaptive MoE, after that, we use the `round` operator to discretize the rank for the remaining training.

Lightweight Temporal Attention. We propose a lightweight temporal attention module designed to explicitly capture temporal dependencies after the self-attention layer. Since the FFN layers in the Transformer serve as mixers along the final dimension of the input sequence [76, 77],

which corresponds to the temporal dimension in our framework, we introduce a new FFN layer consisting of a projection-down layer with the ratio of 6, a nonlinearity, and a corresponding projection-up layer to achieve efficient modeling. Moreover, we integrate a 1D rank-adaptive MoE (RA-MoE) layer, empowering adaptive capacity for multi-discipline learning. The resulting output is then added to the original sequence \mathbf{x} .

Furthermore, in contrast to prior approaches such as the SE module [22] and TAU module [57], which initialize their parameters randomly, we employ a zero-initialization strategy for the second MLP layer within the newly introduced FFN to preserve the pre-trained state of the original Transformer FFN layers and enable more stable optimization. More formally, for the input sequence $\mathbf{x} \in \mathbb{R}^{N \times L}$, Let $\mathbf{x}' = \text{AVGPOOL}(\mathbf{x})$, where $\mathbf{x}' \in \mathbb{R}^{1 \times L}$:

$$\begin{aligned} \mathbf{o} &= \text{FFN}(\mathbf{x}') + \text{RA-MoE}_{1D}(\mathbf{x}') \\ \mathbf{x} &= \mathbf{x} + \text{SIGMOID}(\mathbf{o}). \end{aligned} \quad (11)$$

4. Experiments

4.1. Experimental Setup

Datasets. We quantitatively evaluate our model on the following disciplines with both synthetic and real-world scenarios datasets: **(i) Traffic Control**, including TaxiBJ [80], and Traffic4Cast [9] datasets. **(ii) Trajectory Prediction and Robot Action Planning**, including Moving MNIST [53], BAIR [8], Human3.1M [25], and KTH Action [50] datasets. **(iii) Driving Scene Prediction**, including Cityscapes [6] and KITTI [14] datasets. **(iv) Weather Forecasting**, including SEVIR [63] and ENSO [60] datasets. We summarize the statistics of the above datasets in Tab. 1, including the number of training samples N_{train} and the number of testing samples N_{test} .

Evaluation Metrics. We employ Structure Similarity Index Measure (SSIM), and Peak Signal to Noise Ratio (PSNR) to evaluate the quality of predictions. SSIM measures the similarity of structural information within the spatial neighborhoods, and PSNR is an expression for the ratio between the maximum possible power of a signal and the power of distorted noise. Notably, for weather forecast tasks, we adopt the Critical Success Index (CSI) for the SEVIR dataset and the three-month-moving-averaged Nino3.4 index (NINO) for ENSO dataset.

Implementation Details. UniSTD is implemented using the PyTorch framework. We train all the models for 90 epochs with a mini-batch size of 16, employing the AdamW optimizer configured with a learning rate of 0.01 and weight decay of 0.05. We utilize the standard Vision Transformer architecture (ViT base), comprising 12 layers, an embedding dimension (L) of 768, and a MLP expansion ratio of 4. Each self-attention layer contains 12 attention heads. If the

Table 1. Statistics of the datasets used in experiments. Each dataset has different input/output lengths and dimensions.

Dataset	N_{train}	N_{test}	(C, H, W)	T_{input}	T_{output}
KITTI	9209	2198	(3, 128, 160)	10	10
BAIR	38937	256	(3, 64, 64)	2	10
Cityscapes	8925	1525	(3, 128, 128)	2	5
TaxiBJ	20461	500	(2, 32, 32)	4	4
SEVIR	44760	12144	(1, 384, 384)	13	12
MMNIST	10000	10000	(1, 64, 64)	10	10
KTH Action	8488	5041	(1, 128, 128)	10	10
Human	73404	8582	(3, 256, 256)	4	4
Traffic4Cast	35840	4508	(8, 128, 112)	9	3
ENSO	52350	1679	(1, 48, 48)	12	14

encoder output dimensionality does not match the embedded dimension required by the Transformer, an additional linear projection layer is employed to align the dimensions accordingly. Rank-adaptive MoE modules are integrated into the self-attention layers for the query (\mathbf{Q}), key (\mathbf{K}), value (\mathbf{V}), and projection (Proj) matrices, as well as within the newly introduced temporal attention layer. The number of experts is set to 6 for the \mathbf{Q} , \mathbf{K} , and \mathbf{V} matrices, while the Proj matrices and temporal attention layer utilize 2 experts each. The initial rank for each MoE layer is fixed at 4.5, and the hyperparameter β is set to 1.

4.2. Main Results

Multi-discipline Results. Tab. 2 shows multi-discipline results of the proposed UniSTD method and other baselines including TAU [57], SimVP [12], SimVPv2 [56], and EarthFormer [10] across diverse spatiotemporal prediction tasks. The results are reported in terms of PSNR, SSIM, CSI, and NINO, where higher values indicate better performance.

For the TaxiBJ dataset, the proposed UniSTD method achieves a PSNR of 39.6 and an SSIM of 0.98, significantly outperforming all baseline models. The next-best-performing model, SimVP, achieves a PSNR of 29.7 and an SSIM of 0.75. This represents a substantial improvement of approximately 33% in PSNR and 30% in SSIM, highlighting the ability of UniSTD to model spatiotemporal dependencies effectively in traffic control scenarios. Similarly, for the Traffic4Cast dataset, UniSTD achieves a PSNR of 30.6 and an SSIM of 0.92. In the BAIR and Human3.1M datasets, which are pivotal for trajectory prediction and robot action planning, UniSTD again demonstrates outstanding performance. For the BAIR dataset, UniSTD attains a PSNR of 20.3 and an SSIM of 0.86, outperforming all other models. The best-performing baseline, EarthFormer, achieves a PSNR of 16.3 and an SSIM of 0.61, highlighting an improvement of 25% in PSNR and 41% in SSIM. Similarly, for Human3.1M, UniSTD achieves a PSNR of 33.2 and an SSIM of 0.98, significantly surpassing

Table 2. Main results of UnSTD. Both baselines and UnSTD are trained on the specific spatiotemporal datasets with one model. SimVP_{5 Tasks} indicates that one SimVP model is trained on 3 datasets jointly. PSNR&SSIM: higher is better.

Model	Traffic Control				Trajectory Prediction and Robot Action Planning								Driving Scene Prediction				Weather Forecasting	
	TaxiBJ		Traffic4Cast		MMNIST		BAIR		Human3.1M		KITI		Cityscapes		KITTI		SEVIR	ENSO
	PSNR	SSIM	PSNR	SSIM	PSNR	SSIM	PSNR	SSIM	PSNR	SSIM	PSNR	SSIM	PSNR	PSNR	PSNR	PSNR	CSI	NINO
SimVPv1 _{3 Tasks}	-	23.5	0.05	-	-	-	-	9.8	0.32	-	14.3	0.27	-	-	-	-	-	-
SimVPv2 _{3 Tasks}	24.6	0.56	-	-	-	15.7	0.53	22.4	0.88	-	-	-	-	-	-	-	-	-
SimVPv2 _{3 Tasks}	-	23.7	0.08	-	-	-	-	17.0	0.56	-	12.4	0.18	-	-	-	-	-	-
SimVPv2 _{5 Tasks}	20.4	0.43	-	-	-	12.1	0.34	17.6	0.73	-	14.7	0.46	-	0.32	-	-	-	-
TAU _{3 Tasks}	28.2	0.72	-	-	-	16.5	0.57	21.3	0.84	-	-	-	-	-	-	-	-	-
TAU _{3 Tasks}	30.5	0.78	-	-	-	-	-	22.4	0.86	-	18.9	0.59	-	-	-	-	-	-
TAU _{3 Tasks}	-	-	-	-	-	16.7	0.59	21.2	0.84	-	18.6	0.57	-	-	-	-	-	-
TAU _{3 Tasks}	-	23.8	0.08	-	-	-	-	17.4	0.31	-	-	13.5	0.17	-	-	-	-	-
Eformer _{3 Tasks}	23.2	0.58	-	-	-	-	-	15.2	0.6	-	19.3	0.63	-	-	-	-	-	-
Eformer _{3 Tasks}	23.3	0.60	-	-	-	12.9	0.38	-	-	-	17.2	0.57	-	-	-	-	-	-
Eformer _{3 Tasks}	-	24.0	0.83	-	-	-	-	16.8	0.74	-	-	10.9	0.32	-	-	-	-	-
Eformer _{5 Tasks}	20.8	0.41	-	-	-	12.0	0.32	15.0	0.69	-	14.1	0.41	-	0.30	-	-	-	-
Ours_{10 Tasks}	39.6	0.98	30.6	0.92	20.5	0.90	20.3	0.86	33.2	0.98	28.4	0.92	27.4	0.89	17.2	0.61	0.41	0.72

Table 3. Task-wise comparison of our unified model and the single task baselines.

Task	Model	PSNR	SSIM
TaxiBJ	Ours	39.6	0.9825
	TAU	39.3 (-0.3)	0.9813 (-0.0012)
	SimVP	39.2 (-0.4)	0.9820 (-0.0005)
	SimVPv2	39.2 (-0.4)	0.9812 (-0.0013)
	Earthformer	38.9 (-0.7)	0.9790 (-0.0035)
	MCVD	36.4 (-2.9)	0.9676 (-0.0149)
Cityscapes	Ours	27.4	0.8874
	TAU	26.4 (-1.0)	0.8660 (-0.0214)
	SimVP	26.5 (-0.9)	0.8717 (-0.0157)
	SimVPv2	26.7 (-0.7)	0.8738 (-0.0136)
	MCVD	19.1 (-8.3)	0.8165 (-0.0709)

the performance of the next-best model, TAU_{3 Tasks}, which achieves a PSNR of 23.7 and an SSIM of 0.89. In driving scene prediction tasks, UnSTD also achieves remarkable results. For example, UnSTD delivers a PSNR of 27.4 and an SSIM of 0.89 on Cityscapes, far outperforming the best-performing baseline, TAU_{3 Tasks}, which achieves a PSNR of 19.6 and an SSIM of 0.59. This reflects the UniSTD’s capability to understand complex spatiotemporal interactions in urban driving scenarios with unified modeling. On the KITTI dataset, UnSTD achieves a PSNR of 17.2 and

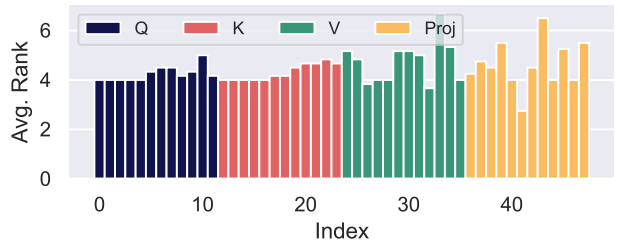


Figure 4. Visualization of the average rank across selected layers (Q, K, V and Proj) in MoEs.

an SSIM of 0.61, surpassing the next-best baseline Earthformer. For the weather forecasting tasks, UnSTD demonstrates consistently better results, e.g., achieving a CSI of 0.41 while the baselines have only about 0.3 on SEVIR.

Compared to Single-task Baseline. The task-wise comparison in Tab 3 highlights the superior performance of our unified model on TaxiBJ and Cityscapes datasets. On TaxiBJ, our model achieves the highest PSNR (39.6) and SSIM (0.9825), significantly outperforming MCVD, which lags with a PSNR of 36.4 and an SSIM of 0.9676. On Cityscapes, our model also leads with a PSNR of 27.4 and an SSIM of 0.8874, showing a notable margin over MCVD’s PSNR of 19.1 and SSIM of 0.8165. These results emphasize the effectiveness of our unified approach, showing that *joint training across multiple tasks could provide cross-task learning benefits*.

Furthermore, we have observed the inconsistent performance of existing methods across various tasks, i.e., the TAU is the best baseline for TaxiBJ but not for Cityscapes,

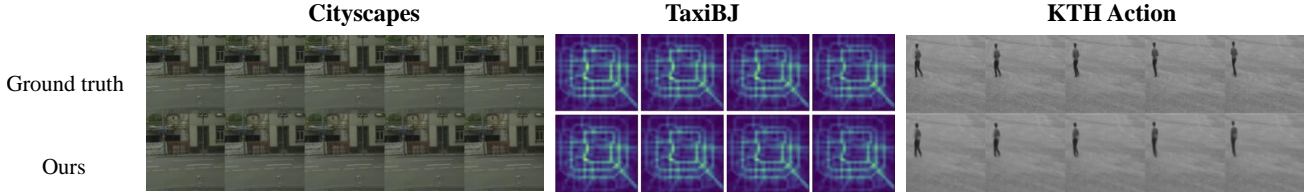


Figure 5. Visualization of the prediction results using a shared model.

Table 4. Effectiveness of proposed Rank-adaptive MoE (AdaMoE) scheme and temporal attention (TAtn.) technique. To save costs, we train the model with 4 tasks. We report the PSNR (higher is better) here.

AdaMoE	TAtn.	BAIR	KTH	Cityscapes	TaxiBJ
✓	✓	20.2	28.2	27.4	39.5
✓	✗	20.1 (-0.1)	27.7 (-0.5)	26.7 (-0.7)	39.4 (-0.1)
✗	✗	20.1 (-0.1)	27.3 (-0.9)	26.2 (-1.2)	39.2 (-0.3)

and Earthformer, the model designed for Earth system forecasting performs second worst for Cityscapes. These observations reveal that the *existing works heavily rely on task-specific knowledge for designing the architecture which leads to limited generality and cannot be directly applied to other tasks.*

4.3. Visualization

Rank-adaptive MoE. Fig. 4 illustrates the average rank of MoEs across selected dense layers (**Q**, **K**, **V**, and **Proj**), where the initial rank of each layer is set to 4.5. Notably, **Q** and **K** exhibit stable rank assignments, with earlier layers predominantly ranked around 4, while later layers receive higher ranks. In contrast, **V** and **Proj** display markedly different patterns, with each layer assigned distinct ranks. This aligns with the observations in Fig. 3, where the norm of **V** is more pronounced and distinctive.

Model Prediction. Fig. 5 shows the visualization of predicted frames using our once-for-all model. Despite very large differences between inputs (such as TaxiBJ for traffic control and Cityscapes for autonomous driving), the models still achieve accurate results, which further demonstrates the effectiveness of our proposed method.

4.4. Ablation Study

Effectiveness of Proposed Method. Tab. 4 evaluates the effectiveness of the proposed Rank-adaptive Mixture-of-Experts (AdaMoE) and Temporal Attention (Temp Attn.) techniques using PSNR (higher is better) across four tasks. The configuration integrating both AdaMoE and Temp Attn. consistently achieves the highest PSNR, highlighting their combined efficacy. For instance, on the KTH dataset, the full model achieves a PSNR of 28.2, surpassing configurations without Temp Attn. (27.7) or without both techniques (27.3). Disabling Temp Attn. while retaining

Table 5. Performance of initialization scheme.

Init. Scheme	BAIR		KTH		Cityscapes	
	PSNR	SSIM	PSNR	SSIM	PSNR	SSIM
Random	20.1	0.85	27.1	0.90	26.7	0.87
LAION [49]	20.2	0.86	28.1	0.92	27.1	0.88
CLIP [46]	20.2	0.86	28.2	0.92	27.4	0.89

AdaMoE results in a moderate decline, with the Cityscapes PSNR dropping from 27.4 to 26.7. The baseline model, devoid of both techniques, performs the worst, with PSNR values such as 39.2 on TaxiBJ compared to 39.5 for the full configuration. These results underscore AdaMoE’s role in adaptively managing model complexity and Temp Attn.’s capability to capture temporal dependencies, demonstrating their complementary contributions to enhanced model performance.

Performance of initialization scheme. In Tab. 5, we show the advantages of pre-trained (*i.e.*, advantages of the task-agnostic pretraining) initialization schemes across three datasets. For BAIR, both LAION [49] and CLIP [46] offer slight improvements over random initialization. On the KTH dataset, pre-trained schemes show more significant benefits, with CLIP achieving the best results (PSNR of 28.2, SSIM of 0.92) compared to random initialization (27.1, 0.90). Similarly, for Cityscapes, CLIP achieves the highest performance (PSNR of 27.4, SSIM of 0.89) over random (26.7, 0.87). These results demonstrate that pre-trained models, particularly CLIP, provide a more robust starting point for spatiotemporal tasks. In this paper, we choose CLIP weight as our initialization scheme.

5. Conclusion

We address the limitations of existing spatiotemporal models by proposing a unified framework and spatiotemporal decoupling modeling. UniSTD leverages a standard Transformer backbone with task-agnostic pretraining and task-specific fine-tuning, ensuring cross-task generality. The decoupling modeling introduces a rank-adaptive mixture-of-expert mechanism and a lightweight temporal module to handle spatial and temporal dependencies. We hope these contributions can advance the field toward general-purpose spatio-temporal learning, reducing reliance on task-specific designs while enhancing adaptability and efficiency.

Acknowledgements. This work is supported partially by the JC STEM Lab of AI for Science and Engineering, funded by The Hong Kong Jockey Club Charities Trust, the Research Grants Council of Hong Kong (Project No. CUHK14213224), the National Natural Science Foundation of China (Grant No. 62306261), and The Shun Hing Institute of Advanced Engineering (SHIAE) (Grant No. 8115074).

References

- [1] Vamsi Aribandi, Yi Tay, Tal Schuster, Jinfeng Rao, Huaixiu Steven Zheng, Sanket Vaibhav Mehta, Honglei Zhuang, Vinh Q Tran, Dara Bahri, Jianmo Ni, et al. Ext5: Towards extreme multi-task scaling for transfer learning. *arXiv preprint arXiv:2111.10952*, 2021. 3
- [2] Mohammad Babaeizadeh, Mohammad Taghi Saffar, Suraj Nair, Sergey Levine, Chelsea Finn, and Dumitru Erhan. Fitvid: Overfitting in pixel-level video prediction. *arXiv preprint arXiv:2106.13195*, 2021. 1
- [3] Tom Brown, Benjamin Mann, Nick Ryder, Melanie Subbiah, Jared D Kaplan, Prafulla Dhariwal, Arvind Neelakantan, Pranav Shyam, Girish Sastry, Amanda Askell, et al. Language models are few-shot learners. *Advances in neural information processing systems*, 33:1877–1901, 2020. 2, 3
- [4] Rich Caruana. Multitask learning. *Machine learning*, 28: 41–75, 1997. 3
- [5] Yuanzheng Ci, Yizhou Wang, Meilin Chen, Shixiang Tang, Lei Bai, Feng Zhu, Rui Zhao, Fengwei Yu, Donglian Qi, and Wanli Ouyang. Unihcp: A unified model for human-centric perceptions. In *Proceedings of the IEEE/CVF Conference on Computer Vision and Pattern Recognition*, pages 17840–17852, 2023. 3
- [6] Marius Cordts, Mohamed Omran, Sebastian Ramos, Timo Rehfeld, Markus Enzweiler, Rodrigo Benenson, Uwe Franke, Stefan Roth, and Bernt Schiele. The cityscapes dataset for semantic urban scene understanding. In *Proceedings of the IEEE conference on computer vision and pattern recognition*, pages 3213–3223, 2016. 6
- [7] Alexey Dosovitskiy, Lucas Beyer, Alexander Kolesnikov, Dirk Weissenborn, Xiaohua Zhai, Thomas Unterthiner, Mostafa Dehghani, Matthias Minderer, Georg Heigold, Sylvain Gelly, et al. An image is worth 16x16 words: Transformers for image recognition at scale. In *International Conference on Learning Representations*, 2020. 1, 2
- [8] Frederik Ebert, Chelsea Finn, Alex X Lee, and Sergey Levine. Self-supervised visual planning with temporal skip connections. *CoRL*, 12(16):23, 2017. 6
- [9] Christian Eichenberger, Moritz Neun, Henry Martin, Pedro Herruzo, Markus Spanring, Yichao Lu, Sungbin Choi, Vsevolod Konyakhin, Nina Lukashina, Aleksei Shpilman, et al. Traffic4cast at neurips 2021-temporal and spatial few-shot transfer learning in gridded geo-spatial processes. In *NeurIPS 2021 Competitions and Demonstrations Track*, pages 97–112. PMLR, 2022. 6
- [10] Zhihan Gao, Xingjian Shi, Hao Wang, Yi Zhu, Yuyang Bernie Wang, Mu Li, and Dit-Yan Yeung. Earthformer: Exploring space-time transformers for earth system forecasting. *Advances in Neural Information Processing Systems*, 35:25390–25403, 2022. 1, 2, 3, 6
- [11] Zhangyang Gao, Cheng Tan, Lirong Wu, and Stan Z. Li. Simvp: Simpler yet better video prediction. In *Proceedings of the IEEE/CVF Conference on Computer Vision and Pattern Recognition (CVPR)*, pages 3170–3180, 2022. 2, 3
- [12] Zhangyang Gao, Cheng Tan, Lirong Wu, and Stan Z Li. Simvp: Simpler yet better video prediction. In *Proceedings of the IEEE/CVF conference on computer vision and pattern recognition*, pages 3170–3180, 2022. 6
- [13] Yuying Ge, Sijie Zhao, Jinguo Zhu, Yixiao Ge, Kun Yi, Lin Song, Chen Li, Xiaohan Ding, and Ying Shan. Seed-x: Multimodal models with unified multi-granularity comprehension and generation. *arXiv preprint arXiv:2404.14396*, 2024. 3
- [14] Andreas Geiger, Philip Lenz, Christoph Stiller, and Raquel Urtasun. Vision meets robotics: The kitti dataset. *The International Journal of Robotics Research*, 32(11):1231–1237, 2013. 6
- [15] Vincent Le Guen and Nicolas Thome. Disentangling physical dynamics from unknown factors for unsupervised video prediction. In *Proceedings of the IEEE/CVF Conference on Computer Vision and Pattern Recognition*, pages 11474–11484, 2020. 1
- [16] Jiaming Han, Kaixiong Gong, Yiyuan Zhang, Jiaqi Wang, Kaipeng Zhang, Dahua Lin, Yu Qiao, Peng Gao, and Xiangyu Yue. Onellm: One framework to align all modalities with language. In *Proceedings of the IEEE/CVF Conference on Computer Vision and Pattern Recognition*, pages 26584–26595, 2024. 2
- [17] Kaiming He, Xiangyu Zhang, Shaoqing Ren, and Jian Sun. Deep residual learning for image recognition. In *Proceedings of the IEEE/CVF Conference on Computer Vision and Pattern Recognition*, pages 770–778, 2016. 1
- [18] Kaiming He, Georgia Gkioxari, Piotr Dollár, and Ross Girshick. Mask r-cnn. In *Proceedings of the IEEE/CVF Conference on Computer Vision and Pattern Recognition*, pages 2961–2969, 2017. 1
- [19] Jonathan Ho, Ajay Jain, and Pieter Abbeel. Denoising diffusion probabilistic models. *Advances in neural information processing systems*, 33:6840–6851, 2020. 1
- [20] Sepp Hochreiter and Jürgen Schmidhuber. Long short-term memory. *Neural computation*, 9(8):1735–1780, 1997. 1
- [21] Edward J Hu, Phillip Wallis, Zeyuan Allen-Zhu, Yuanzhi Li, Shean Wang, Lu Wang, Weizhu Chen, et al. Lora: Low-rank adaptation of large language models. In *International Conference on Learning Representations*. 4
- [22] Jie Hu, Li Shen, and Gang Sun. Squeeze-and-excitation networks. In *Proceedings of the IEEE conference on computer vision and pattern recognition*, pages 7132–7141, 2018. 6
- [23] Ronghang Hu and Amanpreet Singh. Unit: Multimodal multitask learning with a unified transformer. In *Proceedings of the IEEE/CVF International Conference on Computer Vision*, pages 1439–1449, 2021. 3
- [24] Gabriel Ilharco, Mitchell Wortsman, Ross Wightman, Cade Gordon, Nicholas Carlini, Rohan Taori, Achal Dave,

- Vaishaal Shankar, Hongseok Namkoong, John Miller, Hananeh Hajishirzi, Ali Farhadi, and Ludwig Schmidt. Openclip, 2021. If you use this software, please cite it as below. 2
- [25] Catalin Ionescu, Dragos Papava, Vlad Olaru, and Cristian Sminchisescu. Human3.6m: Large scale datasets and predictive methods for 3d human sensing in natural environments. *IEEE transactions on pattern analysis and machine intelligence*, 36(7):1325–1339, 2013. 6
- [26] Andrew Jaegle, Felix Gimeno, Andy Brock, Oriol Vinyals, Andrew Zisserman, and Joao Carreira. Perceiver: General perception with iterative attention. In *International conference on machine learning*, pages 4651–4664. PMLR, 2021. 3
- [27] Shibo Jie, Haoqing Wang, and Zhi-Hong Deng. Revisiting the parameter efficiency of adapters from the perspective of precision redundancy. In *Proceedings of the IEEE/CVF International Conference on Computer Vision*, pages 17217–17226, 2023. 4
- [28] Beibei Jin, Yu Hu, Qiankun Tang, Jingyu Niu, Zhiping Shi, Yinhe Han, and Xiaowei Li. Exploring spatial-temporal multi-frequency analysis for high-fidelity and temporal-consistency video prediction. In *Proceedings of the IEEE/CVF Conference on Computer Vision and Pattern Recognition*, pages 4554–4563, 2020. 1
- [29] Lukasz Kaiser, Aidan N Gomez, Noam Shazeer, Ashish Vaswani, Niki Parmar, Llion Jones, and Jakob Uszkoreit. One model to learn them all. *arXiv preprint arXiv:1706.05137*, 2017. 3
- [30] Alexander Kirillov, Eric Mintun, Nikhila Ravi, Hanzi Mao, Chloe Rolland, Laura Gustafson, Tete Xiao, Spencer Whitehead, Alexander C Berg, Wan-Yen Lo, et al. Segment anything. In *Proceedings of the IEEE/CVF International Conference on Computer Vision*, pages 4015–4026, 2023. 1
- [31] Iasonas Kokkinos. Ubernet: Training a universal convolutional neural network for low-, mid-, and high-level vision using diverse datasets and limited memory. In *Proceedings of the IEEE conference on computer vision and pattern recognition*, pages 6129–6138, 2017. 3
- [32] Alexander Kolesnikov, André Susano Pinto, Lucas Beyer, Xiaohua Zhai, Jeremiah Harmsen, and Neil Houlsby. Uvit: A unified modeling approach for vision with learned guiding codes. *arXiv preprint arXiv:2205.10337*, 2022. 3
- [33] Sangmin Lee, Hak Gu Kim, Dae Hwi Choi, Hyung-II Kim, and Yong Man Ro. Video prediction recalling long-term motion context via memory alignment learning. In *Proceedings of the IEEE/CVF Conference on Computer Vision and Pattern Recognition*, pages 3054–3063, 2021. 3
- [34] Junnan Li, Dongxu Li, Caiming Xiong, and Steven Hoi. Blip: Bootstrapping language-image pre-training for unified vision-language understanding and generation. In *International conference on machine learning*, pages 12888–12900. PMLR, 2022. 1
- [35] Junnan Li, Dongxu Li, Silvio Savarese, and Steven Hoi. Blip-2: Bootstrapping language-image pre-training with frozen image encoders and large language models. In *International conference on machine learning*, pages 19730–19742. PMLR, 2023. 2
- [36] Wei-Hong Li, Xialei Liu, and Hakan Bilen. Learning multiple dense prediction tasks from partially annotated data. In *Proceedings of the IEEE/CVF Conference on Computer Vision and Pattern Recognition*, pages 18879–18889, 2022. 3
- [37] Wei-Hong Li, Xialei Liu, and Hakan Bilen. Universal representations: A unified look at multiple task and domain learning. *International Journal of Computer Vision*, 132(5):1521–1545, 2024. 3
- [38] Yanwei Li, Yuechen Zhang, Chengyao Wang, Zhisheng Zhong, Yixin Chen, Ruihang Chu, Shaoteng Liu, and Jiaya Jia. Mini-gemini: Mining the potential of multi-modality vision language models. *arXiv preprint arXiv:2403.18814*, 2024. 3
- [39] Jianming Liang, Guanglu Song, Biao Leng, and Yu Liu. Unifying visual perception by dispersible points learning. *arXiv preprint arXiv:2208.08630*, 2022. 3
- [40] Haotian Liu, Chunyuan Li, Qingyang Wu, and Yong Jae Lee. Visual instruction tuning. *Advances in neural information processing systems*, 36, 2024. 2
- [41] William Lotter, Gabriel Kreiman, and David Cox. Deep predictive coding networks for video prediction and unsupervised learning. In *International Conference on Learning Representations*, 2017. 3
- [42] Ishan Misra, Abhinav Shrivastava, Abhinav Gupta, and Martial Hebert. Cross-stitch networks for multi-task learning. In *Proceedings of the IEEE conference on computer vision and pattern recognition*, pages 3994–4003, 2016. 3
- [43] Xuesong Nie, Yunfeng Yan, Siyuan Li, Cheng Tan, Xi Chen, Haoyuan Jin, Zhihang Zhu, Stan Z Li, and Donglian Qi. Wavelet-driven spatiotemporal predictive learning: Bridging frequency and time variations. In *Proceedings of the AAAI Conference on Artificial Intelligence*, pages 4334–4342, 2024. 3
- [44] Alec Radford. Improving language understanding by generative pre-training. 2018. 2
- [45] Alec Radford, Jeffrey Wu, Rewon Child, David Luan, Dario Amodei, Ilya Sutskever, et al. Language models are unsupervised multitask learners. *OpenAI blog*, 1(8):9, 2019. 2
- [46] Alec Radford, Jong Wook Kim, Chris Hallacy, Aditya Ramesh, Gabriel Goh, Sandhini Agarwal, Girish Sastry, Amanda Askell, Pamela Mishkin, Jack Clark, et al. Learning transferable visual models from natural language supervision. In *International conference on machine learning*, pages 8748–8763. PMLR, 2021. 8
- [47] Shaoqing Ren, Kaiming He, Ross Girshick, and Jian Sun. Faster r-cnn: Towards real-time object detection with region proposal networks. *Advances in Neural Information Processing Systems*, 28:91–99, 2015. 1
- [48] S Ruder. An overview of multi-task learning in deep neural networks. *arXiv preprint arXiv:1706.05098*, 2017. 3
- [49] Christoph Schuhmann, Richard Vencu, Romain Beaumont, Robert Kaczmarczyk, Clayton Mullis, Aarush Katta, Theo Coombes, Jenia Jitsev, and Aran Komatsuzaki. Laion-400m: Open dataset of clip-filtered 400 million image-text pairs. *arXiv preprint arXiv:2111.02114*, 2021. 8

- [50] Christian Schuldt, Ivan Laptev, and Barbara Caputo. Recognizing human actions: a local svm approach. In *Proceedings of the 17th International Conference on Pattern Recognition, 2004. ICPR 2004.*, pages 32–36. IEEE, 2004. 6
- [51] Xingjian Shi, Zhoung Chen, Hao Wang, Dit-Yan Yeung, Wai-Kin Wong, and Wang-chun Woo. Convolutional lstm network: A machine learning approach for precipitation nowcasting. *Advances in Neural Information Processing Systems*, 28, 2015. 1, 2, 3
- [52] Jiaming Song, Chenlin Meng, and Stefano Ermon. Denoising diffusion implicit models. *arXiv preprint arXiv:2010.02502*, 2020. 1
- [53] Nitish Srivastava, Elman Mansimov, and Ruslan Salakhudinov. Unsupervised learning of video representations using lstms. In *International conference on machine learning*, pages 843–852. PMLR, 2015. 6
- [54] Jiahao Su, Wonmin Byeon, Jean Kossaifi, Furong Huang, Jan Kautz, and Anima Anandkumar. Convolutional tensor-train lstm for spatio-temporal learning. *Advances in Neural Information Processing Systems*, 33:13714–13726, 2020. 3
- [55] Quan Sun, Qiyang Yu, Yufeng Cui, Fan Zhang, Xiaosong Zhang, Yuezhe Wang, Hongcheng Gao, Jingjing Liu, Tiejun Huang, and Xinlong Wang. Generative pretraining in multi-modality. *arXiv preprint arXiv:2307.05222*, 2023. 3
- [56] Cheng Tan, Zhangyang Gao, Siyuan Li, and Stan Z Li. Simvp: Towards simple yet powerful spatiotemporal predictive learning. *arXiv preprint arXiv:2211.12509*, 2022. 2, 3, 6
- [57] Cheng Tan, Zhangyang Gao, Lirong Wu, Yongjie Xu, Jun Xia, Siyuan Li, and Stan Z Li. Temporal attention unit: Towards efficient spatiotemporal predictive learning. In *Proceedings of the IEEE/CVF Conference on Computer Vision and Pattern Recognition*, pages 18770–18782, 2023. 1, 2, 3, 6
- [58] Cheng Tan, Siyuan Li, Zhangyang Gao, Wenfei Guan, Zedong Wang, Zicheng Liu, Lirong Wu, and Stan Z Li. Opentstl: A comprehensive benchmark of spatio-temporal predictive learning. *Advances in Neural Information Processing Systems*, 36:69819–69831, 2023. 2
- [59] Mingxing Tan and Quoc Le. Efficientnet: Rethinking model scaling for convolutional neural networks. In *International Conference on Machine Learning*, pages 6105–6114. PMLR, 2019. 1
- [60] <https://tianchi.aliyun.com/>. Historical climate observation and stimulation dataset. <https://tianchi.aliyun.com/dataset/98942>. Accessed: 2023-11-17. 6
- [61] Simon Vandenhende, Stamatios Georgoulis, Wouter Van Gansbeke, Marc Proesmans, Dengxin Dai, and Luc Van Gool. Multi-task learning for dense prediction tasks: A survey. *IEEE transactions on pattern analysis and machine intelligence*, 44(7):3614–3633, 2021. 3
- [62] Ashish Vaswani, Noam Shazeer, Niki Parmar, Jakob Uszkoreit, Llion Jones, Aidan N Gomez, Lukasz Kaiser, and Illia Polosukhin. Attention is all you need. *Advances in neural information processing systems*, 30, 2017. 3
- [63] Mark Veillette, Siddharth Samsi, and Chris Mattioli. Sevir: A storm event imagery dataset for deep learning applications in radar and satellite meteorology. *Advances in Neural Information Processing Systems*, 33:22009–22019, 2020. 6
- [64] Ruben Villegas, Dumitru Erhan, Honglak Lee, et al. Hierarchical long-term video prediction without supervision. In *International Conference on Machine Learning*, pages 6038–6046. PMLR, 2018. 1
- [65] Ruben Villegas, Arkanath Pathak, Harini Kannan, Dumitru Erhan, Quoc V Le, and Honglak Lee. High fidelity video prediction with large stochastic recurrent neural networks. *Advances in Neural Information Processing Systems*, 32, 2019. 1
- [66] Vikram Voleti, Alexia Jolicoeur-Martineau, and Chris Pal. Mcvd-masked conditional video diffusion for prediction, generation, and interpolation. *Advances in neural information processing systems*, 35:23371–23385, 2022. 3
- [67] Peng Wang, An Yang, Rui Men, Junyang Lin, Shuai Bai, Zhikang Li, Jianxin Ma, Chang Zhou, Jingren Zhou, and Hongxia Yang. Ofa: Unifying architectures, tasks, and modalities through a simple sequence-to-sequence learning framework. In *International Conference on Machine Learning*, pages 23318–23340. PMLR, 2022. 3
- [68] Yunbo Wang, Mingsheng Long, Jianmin Wang, Zhifeng Gao, and Philip S Yu. Predrnn: Recurrent neural networks for predictive learning using spatiotemporal lstms. *Advances in Neural Information Processing Systems*, 30, 2017. 1, 2, 3
- [69] Yunbo Wang, Zhifeng Gao, Mingsheng Long, Jianmin Wang, and S Yu Philip. Predrnn++: Towards a resolution of the deep-in-time dilemma in spatiotemporal predictive learning. In *International Conference on Machine Learning*, pages 5123–5132. PMLR, 2018.
- [70] Yunbo Wang, Lu Jiang, Ming-Hsuan Yang, Li-Jia Li, Mingsheng Long, and Li Fei-Fei. Eidetic 3d lstm: A model for video prediction and beyond. In *International conference on learning representations*, 2018. 2, 3
- [71] Yunbo Wang, Jianjin Zhang, Hongyu Zhu, Mingsheng Long, Jianmin Wang, and Philip S Yu. Memory in memory: A predictive neural network for learning higher-order non-stationarity from spatiotemporal dynamics. In *Proceedings of the IEEE/CVF Conference on Computer Vision and Pattern Recognition*, pages 9154–9162, 2019.
- [72] Yunbo Wang, Haixu Wu, Jianjin Zhang, Zhifeng Gao, Jianmin Wang, Philip S Yu, and Mingsheng Long. Predrnn: A recurrent neural network for spatiotemporal predictive learning. *arXiv preprint arXiv:2103.09504*, 2021. 1, 3
- [73] Zidong Wang, Zeyu Lu, Di Huang, Tong He, Xihui Liu, Wanli Ouyang, and Lei Bai. Predbench: Benchmarking spatio-temporal prediction across diverse disciplines. *arXiv preprint arXiv:2407.08418*, 2024. 2
- [74] Haixu Wu, Zhiyu Yao, Jianmin Wang, and Mingsheng Long. Motionrnn: A flexible model for video prediction with spacetime-varying motions. In *Proceedings of the IEEE/CVF Conference on Computer Vision and Pattern Recognition*, pages 15435–15444, 2021. 3
- [75] Wei Yu, Yichao Lu, Steve Easterbrook, and Sanja Fidler. Efficient and information-preserving future frame prediction and beyond. In *International Conference on Learning Representations*, 2019. 1

- [76] Weihao Yu, Mi Luo, Pan Zhou, Chenyang Si, Yichen Zhou, Xinchao Wang, Jiashi Feng, and Shuicheng Yan. Metaformer is actually what you need for vision. In *Proceedings of the IEEE/CVF conference on computer vision and pattern recognition*, pages 10819–10829, 2022. [5](#)
- [77] Weihao Yu, Chenyang Si, Pan Zhou, Mi Luo, Yichen Zhou, Jiashi Feng, Shuicheng Yan, and Xinchao Wang. Metaformer baselines for vision. *IEEE Transactions on Pattern Analysis and Machine Intelligence*, 2023. [5](#)
- [78] Yuan Yuan, Jingtao Ding, Jie Feng, Depeng Jin, and Yong Li. Unist: A prompt-empowered universal model for urban spatio-temporal prediction. In *Proceedings of the 30th ACM SIGKDD Conference on Knowledge Discovery and Data Mining*, pages 4095–4106, 2024. [2](#)
- [79] Amir R Zamir, Alexander Sax, Nikhil Cheerla, Rohan Suri, Zhangjie Cao, Jitendra Malik, and Leonidas J Guibas. Robust learning through cross-task consistency. In *Proceedings of the IEEE/CVF conference on computer vision and pattern recognition*, pages 11197–11206, 2020. [3](#)
- [80] Junbo Zhang, Yu Zheng, Dekang Qi, Ruiyuan Li, Xiuwen Yi, and Tianrui Li. Predicting citywide crowd flows using deep spatio-temporal residual networks. *Artificial Intelligence*, 259:147–166, 2018. [6](#)
- [81] Xizhou Zhu, Weijie Su, Lewei Lu, Bin Li, Xiaogang Wang, and Jifeng Dai. Deformable detr: Deformable transformers for end-to-end object detection. *arXiv preprint arXiv:2010.04159*, 2020. [1](#)

UniSTD: Towards Unified Spatio-Temporal Learning across Diverse Disciplines

Supplementary Material

Task	Method	Trainable Params. (\downarrow)
KITTI+Traffic.+KTH	SimVPv1	45.8M
	SimVPv2	35.3M
	TAU	33.9M
	UniSTD (Ours)	18.5M
BAIR+TaxiBJ+Human +City.+KTH+Traffic. +KITTI	SimVPv1	61.7M
	SimVPv2	47.8M
	TAU	45.8M
	UniSTD (Ours)	23.6M

Table 7. Number of trainable Parameters of UniT and baseline.

1. Implementation Details

Architecture. More details about the architectures of UniSTD are shown in Tab. 8. The decoder blocks are the same as the Encoder blocks but with the TransposedConv2d layers to replace the Conv2d layers in the Encoder layers for upsampling the features.

Training Details. We train the model for 90 epochs with the AdamW optimizer for the weights and SGD optimizer for the trainable rank of MoE. For the Adam optimizer, the weight decay is set to $1e-5$, the learning rate is set to $7e-4$ with cosine learning rate scheduler and the first 5 epochs are used for warm-up (using $1e-8$ learning rate). For the SGD optimizer, we enable the Nesterov momentum and set the learning rate to 0.05.

2. Additional Results

Task	Model	PSNR (\uparrow)	SSIM (\uparrow)
BAIR	Ours	20.3	0.86
	TAU	19.8	0.86
	SimVPv1	20.3	0.86
	SimVPv2	19.9	0.85
KTH	Ours	28.4	0.92
	TAU	27.9	0.90
	SimVPv1	27.7	0.90
	SimVPv2	27.9	0.90
MMNIST	Ours	20.5	0.90
	TAU	18.9	0.85
	SimVPv1	19.5	0.88
	SimVPv2	19.0	0.85

Table 6. Task-wise comparison of our unified model and the single task baselines.

More Evaluation Metrics. We provide an additional evaluation metric RMSE in Tab. 10, one can see that our method still yield best performance across various methods.

Task-wise Training Results. In Tab. 6, we show the additional results of our joint trained model compared to the single-task training (independent training) of baselines. Our model shows significant improvements on metrics of both PSNR and SSIM, this further indicates that the joint training can benefit the learning process of each task. We train the baseline using our training settings for fair comparison.

Efficiency Analysis. In Tab. 9 and Tab. 7, we show the computational complexity (FLOPs) and number of trainable parameters of the proposed method and baseline, respectively. On the one hand, long-range spatial modeling of Transformer allows UniSTD to use much smaller spatial dimensions, thus more efficient on mid/large resolution tasks (e.g., SEVIR, Human, etc) in terms of FLOPs. On the other hand, our method uses only about 50% trainable parameters of the baselines while achieving much better performance.

Table 8. Architecture details of UniSTD.

	TaxiBJ	Traffic4Cast	MMNIST	BAIR	Human3.1M	KTH	Cityscapes	KITTI	SEVIR	ENSO
GFLOPs	6.91	26.43	7.36	139.97	31.53	29.89	85.01	37.78	88.76	62.97
Shape: (B*T, C, H, W)	(B*4, 2, 32, 32)	(B*9, 8, 128, 112)	(B*10, 1, 64, 64)	(B*2, 3, 64, 64)	(B*4, 3, 256, 256)	(B*10, 1, 128, 128)	(B*2, 3, 128, 128)	(B*10, 3, 128, 160)	(B*13, 1, 384, 384)	(B*12, 1, 24, 48)
Encoder Block: - Conv2d (stride=1, channels=T) - GroupNorm - SiLU - Conv2d (stride=2, channels=C) - GroupNorm - SiLU	*2	*3	*3	*2	*4	*3	*3	*3	*4	*1
C'=64										
Shape: (B, T*C, H', W')	(B, 256, 8, 8)	(B, 576, 16, 14)	(B, 640, 8, 8)	(B, 128, 16, 16)	(B, 256, 16, 16)	(B, 640, 16, 16)	(B, 128, 16, 16)	(B, 640, 16, 20)	(B, 832, 24, 24)	(B, 768, 12, 24)
Projection Layer: - Conv2d (stride=1, channels=768)	*1	*1	*1	*1	*1	*1	*1	*1	*1	*1
Shape: (B, 768, H', W')	(B, 768, H', W')									
- Reshape	N=H'*W', L=768									
Shape: (B, N, L)	(B, 64, 768)	(B, 224, 768)	(B, 64, 768)	(B, 256, 768)	(B, 256, 768)	(B, 256, 768)	(B, 256, 768)	(B, 320, 768)	(B, 576, 768)	(B, 288, 768)
Backbone: - Transformer Blocks (shared) with Rank-Adaptive MoE and Temp. Attn.	* 12									

Table 9. GFLOPs (lower is better) comparison.

	TaxiBJ	Traffic4Cast	MMNIST	BAIR	Human3.1M	KTH	Cityscapes	KITTI	SEVIR	ENSO
UniSTD (Ours)	6.91	26.43	7.36	139.97	31.53	29.89	<u>85.01</u>	37.78	88.76	62.97
SimVP _{v1}	3.53	40.01	15.15	277.64	231.80	<u>50.06</u>	127.70	<u>62.60</u>	426.92	25.58
SimVP _{v2}	<u>2.54</u>	32.06	12.28	194.77	166.59	64.26	88.79	80.35	398.34	22.82
TAU	2.43	<u>30.62</u>	<u>11.75</u>	<u>185.44</u>	<u>158.83</u>	61.25	84.78	76.59	<u>379.91</u>	21.79

Table 10. RMSE (\downarrow) metrics.

	TaxiBJ	Traffic4Cast	MMNIST	BAIR	Human3.1M	KTH	Cityscapes	KITTI
UniSTD (Ours)	0.54	8.78	6.27	11.54	10.46	5.42	10.82	39.49
SimVP _{3 task}	2.86	-	-	18.79	35.45	-	-	-
TAU _{3 task}	1.69	-	-	-	34.48	-	26.56	76.59
UniST [78]	0.90	-	-	25.76	-	23.36	-	56.95